Available online at www.sciencedirect.com
ScienceDirect
Journal of Power Sources 175 (2008) 526–532
JOURNAL OF POWER SOURCES
www.elsevier.com/locate/jpowsour

Investigating the solid electrolyte interphase using binder-free graphite electrodes

S.-H. Kang [a], D.P. Abraham [a,*], A. Xiao [b], B.L. Lucht [b]

[a] *Chemical Engineering Division, Argonne National Laboratory, 9700 South Cass Avenue, Argonne, IL 60439, USA*
[b] *Department of Chemistry, University of Rhode Island, 51 Lower College Road, Kingston, RI 02881, USA*

Received 9 August 2007; accepted 31 August 2007
Available online 12 September 2007

Abstract

Binder-free (BF) electrodes simplify interpretation of solid electrolyte interphase (SEI) data obtained from studies of graphite surfaces. In this work, we prepared BF-graphite electrodes by electrophoretic deposition (EPD), and the SEI layers formed on the electrode in lithium cells containing $LiPF_6$- and $LiF_2BC_2O_4$-bearing electrolytes were examined by Fourier transform infrared spectroscopy (FTIR) and X-ray photoelectron spectroscopy (XPS). The results showed that the dominant SEI species were lithium alkyl carbonates ($ROCO_2Li$) and lithium alkoxides (ROLi); Li_2CO_3 was conspicuously absent. Trigonal borate oligomers are most likely present in the SEI of graphite samples cycled in $LiF_2BC_2O_4$ electrolyte, while lithium fluorophosphates are present on graphite samples cycled in $LiPF_6$ electrolyte. The SEI layer coverage was greater on graphite samples cycled in $LiF_2BC_2O_4$ electrolyte than in the $LiPF_6$ electrolyte. Our results demonstrate that BF-graphite electrodes prepared by EPD are suitable for the study of SEI layer formed in various electrolyte systems.

Keywords: Electrophoretic deposition; $LiPF_6$; $LiF_2BC_2O_4$; Passivation films

1. Introduction

Graphite is the most widely adopted anode material in commercial lithium-ion batteries. When lithium ions are intercalated into graphite during initial charge of a lithium-ion battery, the electrolyte components reduce (or decompose) to form a passivation film on the graphite surface that is generally called the solid electrolyte interphase (SEI) [1]. This SEI layer plays the important role of protecting the graphite surfaces during subsequent cycling; the composition, morphology, and stability of the SEI are known to critically affect the cycle- and storage-life of a lithium-ion cell [2,3].

The morphology and chemical composition of the graphite SEI layer depend on various factors that include characteristics of electrolyte solvents, composition of lithium salts, and nature of electrolyte additives [4–10]. Because a stable SEI layer at the anode surface is critical to the reliable performance of lithium-ion batteries, a significant number of studies have been conducted over the last two decades to delineate SEI layer characteristics. There is, however, a continuing debate on formation mechanisms and on the composition of the SEI layer present on graphite surfaces in various electrolyte systems. One such debate revolves around the presence of Li_2CO_3 in the graphite SEI that has been reported in some studies [11,12] but not in others [3,8]. Fourier transform infrared spectroscopy (FTIR) and X-ray photoelectron spectroscopy (XPS) are typically used to characterize the SEI layer. One difficulty in performing detailed and conclusive analysis of data from these techniques lies in the presence of inactive components, such as the polyvinylidene difluoride (PVdF) binder used in conventional composite electrodes; data from these components often obscure information arising from chemical species in the SEI layer.

A binder-free (BF) graphite electrode would simplify interpretation of SEI data obtained from studies of electrode surfaces. To this end, several SEI studies have been conducted on highly oriented pyrolytic graphite (HOPG) electrodes [13–15]. However, HOPG electrodes are better suited to studying the SEI on basal planes than on graphite edge planes because of the large basal-to-edge-plane surface-area ratio. Because the SEI formed on graphite edge planes (the sites of lithium

* Corresponding author. Tel.: +1 630 252 4332; fax: +1 630 972 4406.
E-mail address: abraham@cmt.anl.gov (D.P. Abraham).

0378-7753/$ – see front matter © 2007 Elsevier B.V. All rights reserved.
doi:10.1016/j.jpowsour.2007.08.112

intercalation) is important from a practical perspective, the studies on HOPG electrodes are of limited value. Model studies of electrolyte reduction and SEI formation have been conducted on non-graphitic electrodes, such as Pt, Ni, Si, and intermetallic compounds. However, these materials are not appropriate surrogates for graphite because the SEI composition and morphology are different for each compound (or active material).

In this work, we examined and characterized the SEI layers formed on binder-free graphite electrodes fabricated on Cu foil by electrophoretic deposition (EPD). The BF-graphite electrodes were cycled in cells containing electrolytes with two different lithium salts: lithium hexafluoro phosphate ($LiPF_6$) and lithium difluoro(oxalato)borate ($LiF_2BC_2O_4$). $LiPF_6$ is a standard lithium salt used in commercial lithium-ion cells, whereas $LiF_2BC_2O_4$ is attracting attention as an alternative to $LiPF_6$ [16,17]. The $LiF_2BC_2O_4$ salt is also being studied as a functional electrolyte additive [10,18]. FTIR and XPS studies have been conducted to examine the SEI layer formed on the BF-graphite electrodes in these electrolytes.

2. Experimental

2.1. Electrode preparation and initial characterization

The BF-graphite electrodes were prepared by electrophoretic deposition (EPD) [19]. The graphite solution for EPD was prepared by dispersing graphite particles (SFG-6, TIMCAL, $5\,g\,L^{-1}$) in acetonitrile by ultrasonication. Small amounts ($1\,mL\,L^{-1}$) of triethylamine were added to the EPD bath, to form surface charges on the graphite particles. Copper and stainless steel foils (5 cm × 5 cm) were used as cathode and anode, respectively; the distance between the two electrodes was 7 mm. The graphite particles were deposited on the copper foil by applying a dc voltage of 32 V for 60 s to the electrodes. The graphite electrode, thus prepared, was dried in a vacuum oven at ~76 °C to completely remove the residual acetonitrile and triethylamine. The average graphite loading density of the resulting electrode was $\sim 1.7\,mg\,cm^{-2}$. Crystal structure and morphology of the graphite electrode were examined with a Siemens D5000 X-ray diffractometer (Cu Kα radiation) and a high-resolution Hitachi S-4700 scanning electron microscope equipped with a field emission electron source, respectively.

2.2. SEI layer formation

Cell assembly, galvanostatic cycling, and cell disassembly were conducted in an Ar-atmosphere glove box (<1 ppm H_2O, <5 ppm O_2) to prevent any influence of air on the SEI layer formation. Electrochemical testing of the electrode and SEI layer formation were conducted using 2032-type coin cells containing small pieces ($\sim 0.8\,cm^2$) of the BF-graphite electrode, metallic lithium counter electrode, and Celgard 2325 (25-μm-thick) separator. Two different electrolytes were used to study the effect of lithium salts on the SEI layer: 1.2 M $LiPF_6$ in a mixture of ethylene carbonate (EC) and ethylmethyl carbonate (EMC) (3:7, w/w), which will be henceforth referred to as the $LiPF_6$ electrolyte; and 1 M $LiF_2BC_2O_4$ in a mixture of EC and EMC (3:7, w/w), which will be referred to as the $LiF_2BC_2O_4$ electrolyte. The coin cells were cycled between 2.0 and 0 V at a current density of $8\,mA\,g^{-1}$ at room temperature. For the SEI layer formation, only a single lithiation–delithiation cycle was conducted. The cells were then disassembled, and the delithiated graphite electrodes were harvested for SEI examination.

2.3. SEI layer examination

The harvested graphite electrodes were examined, without washing, by FTIR with attenuated total reflection (ATR) and XPS. FTIR-ATR provides information on functional groups present in the top ~1 μm of the graphite electrode without destroying the surface species, whereas XPS provides information on chemical species present in a <5-nm-thick layer on the electrode surface.

The FTIR-ATR measurements were conducted on a Thermo Nicolet IR 300 spectrometer stored in a glove bag that was purged with high-purity Ar. The data were acquired without any sample air exposure, and the spectra, acquired in the ATR mode with the $4\,cm^{-1}$ resolution and 128 total scans, were obtained in triplicate at different spots to avoid possible error and to examine uniformity of the SEI layer.

After the FTIR-ATR studies, the samples were examined by XPS with a PHI 5500 system using Al Kα radiation ($h\nu = 1486.6\,eV$) under ultra-high-vacuum (UHV) conditions. Each sample was exposed to air for a few seconds during insertion into the XPS analysis chamber. The XPS data were acquired at two different spots for each sample. The C 1s, O 1s, F 1s, P 2p, and B 1s spectra were calibrated based on the C 1s graphite peak binding energy at 284 eV.

3. Results and discussion

3.1. Physical and electrochemical characterization

Fig. 1 is a representative XRD pattern from the BF-graphite electrode; only peaks from graphite and Cu (current collector) are seen in the pattern. Fig. 2a and b are representative SEM images from the electrode. The lower magnification image (Fig. 2a) shows that the distribution of graphite particles is relatively uniform; the higher magnification image (Fig. 2b) shows flaky particles, typical of SFG-6 graphite. Fig. 3a and b shows representative C 1s XPS spectra from the BF-graphite electrode and a typical PVdF-bearing composite electrode, respectively. Only graphite peaks are observed in Fig. 3a, whereas PVdF peaks that could obscure data from the SEI are seen in Fig. 3b.

Fig. 4 shows charge–discharge curves of the lithium cells for the first two cycles (Fig. 4a and b) and differential capacity plots for the first cycle (Fig. 4c and d) from the cells containing the $LiPF_6$ (Fig. 4a and c) and $LiF_2BC_2O_4$ (Fig. 4b and d) electrolytes. Capacity changes during the initial 10 cycles of the $LiPF_6$- and $LiF_2BC_2O_4$-electrolyte cells are shown in the insets of Fig. 4a and b, respectively, it is evident that the graphite electrode displays stable cycling characteristics in both electrolytes.

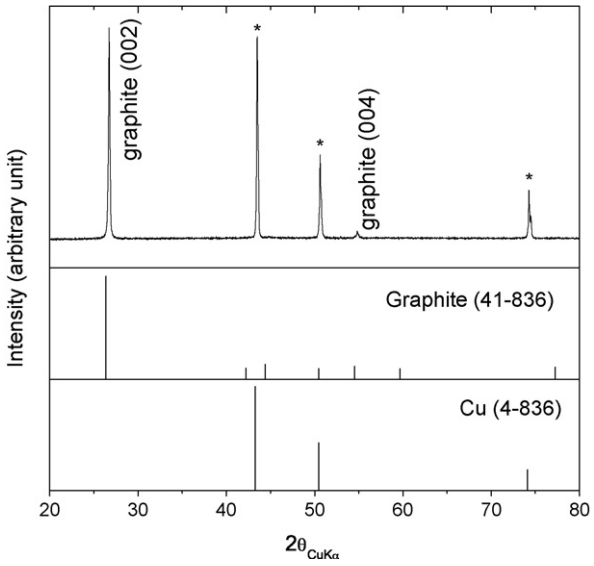

Fig. 1. Representative XRD pattern from fresh BF-graphite electrode shows only graphite and Cu (current collector) peaks.

Both types of Li cells exhibit typical graphite 'staging' behavior below 0.5 V versus Li^+/Li due to the formation of various Li_xC_6 phases ($x = 0.25, 0.33, 0.5, 1$) by lithium intercalation (see Fig. 4c and d). The $LiPF_6$ cell shows a short, irreversible voltage plateau (or a small, irreversible reduction peak) at ~0.7 V versus Li^+/Li during initial lithiation (white arrows in Fig. 4a and c), which can be attributed to the reductive decomposition of carbonate solvents (mostly EC) to form an SEI layer on the graphite surface. A similar peak is observed for the $LiF_2BC_2O_4$ cell but at a slightly higher voltage (~0.9 V vs. Li^+/Li). In addition to the solvent reduction peak, the $LiF_2BC_2O_4$ cell shows a long voltage plateau (or an irreversible differential capacity peak) at ~1.7 V versus Li^+/Li during the first lithiation process (black arrows in Fig. 4b and d). This additional peak has been commonly observed in graphite/Li cells with LiBOB and $LiF_2BC_2O_4$ electrolytes [16,17,20]. Based on the experimental results reported in recent papers [17,21,22], it is believed that the 1.7 V-peak in Fig. 4d is closely related to the oxalate moiety in $F_2BC_2O_4$ anions.

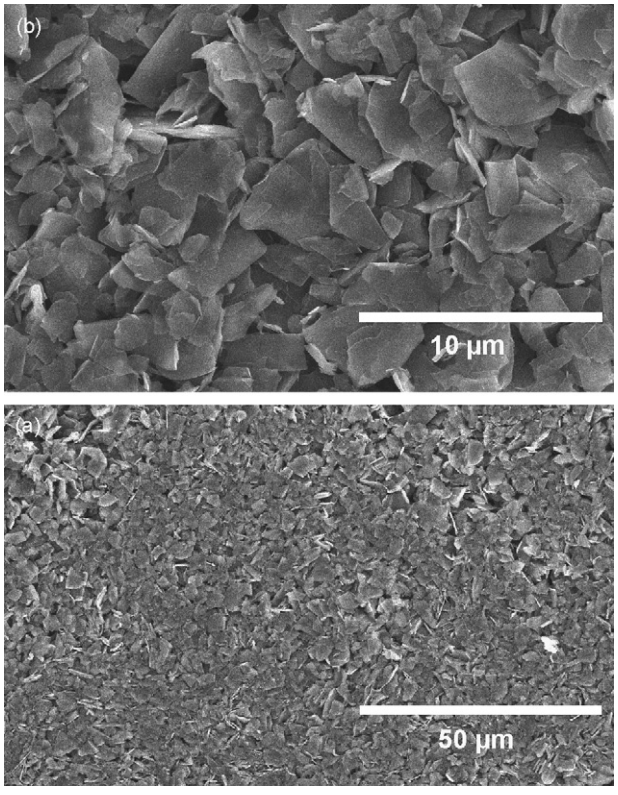

Fig. 2. Representative (a) low- and (b) high-magnification SEM images from fresh BF-graphite electrode.

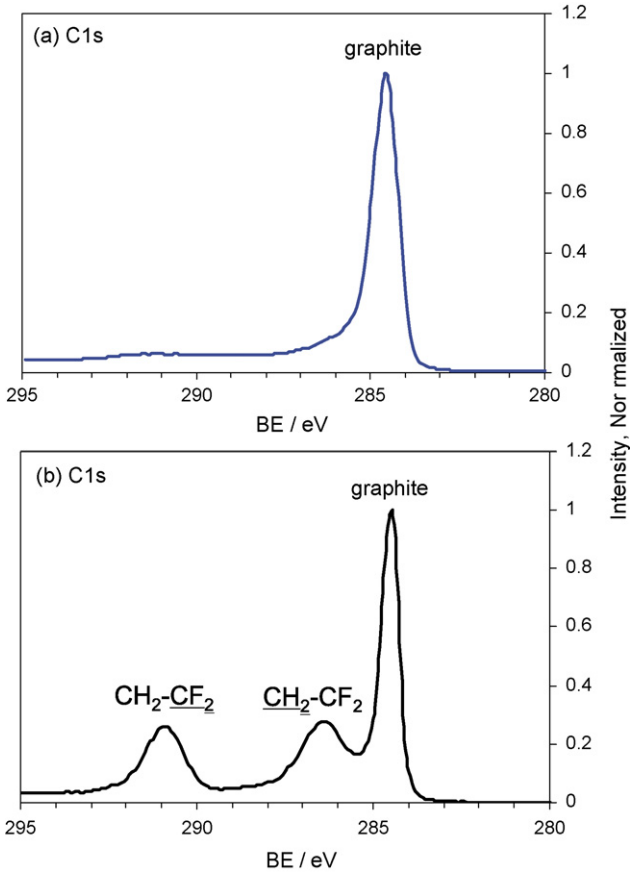

Fig. 3. The C 1s XPS spectra comparing (a) a fresh BF-graphite electrode with (b) a typical fresh composite electrode.

3.2. FTIR-ATR

Fig. 5 shows the FTIR-ATR surface spectra from BF-graphite electrodes, cycled once between 2.0 and 0.0 V, in the $LiPF_6$- and $LiF_2BC_2O_4$-electrolyte cells; the electrodes were examined in the delithiated state. The fresh graphite electrode data, shown for comparison, displays no evidence of functional groups. The spectra from the $LiPF_6$ and $LiF_2BC_2O_4$ cells indicate strong absorptions at 1803 and 1770 cm^{-1} and medium-strong features at 1480, 1160, and 771 cm^{-1} (denoted by ●), which can be assigned to solvated EC:lithium; these absorptions also include contributions from electrolyte residue on the sample surface [8,9,23]. The peaks in both spectra, at 1665, 1391, 1334, and 1071 cm^{-1} (denoted by *), appear to arise from lithium ethy-

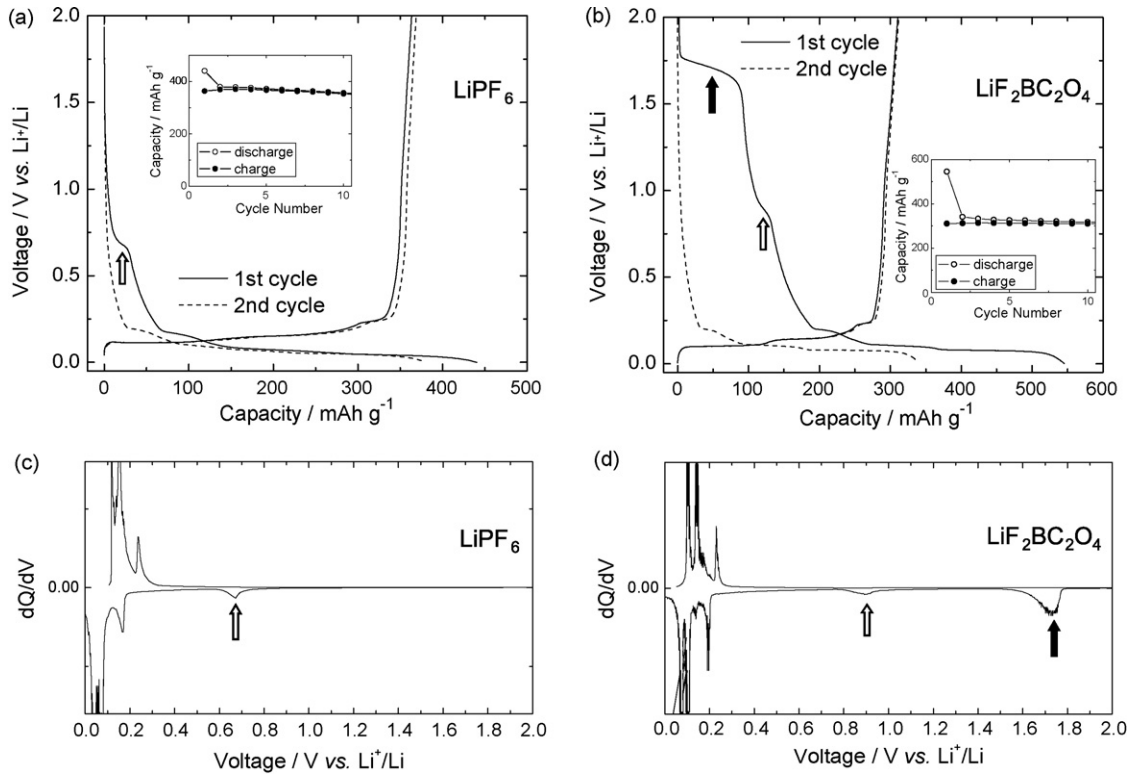

Fig. 4. Electrochemical data from the BF-graphite electrode cycled in $LiPF_6$-bearing cells (a) and (c) and $LiF_2BC_2O_4$-bearing cells (b) and (d).

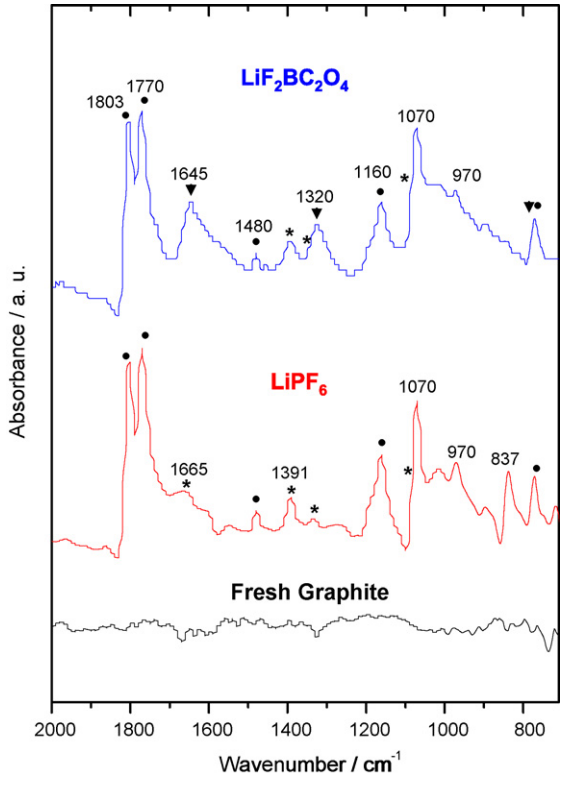

Fig. 5. FTIR data from a fresh BF-graphite electrode, and from the electrodes cycled in $LiPF_6$- and $LiF_2BC_2O_4$-electrolyte cells.

lene dicarbonate (LEDC) or a related species such as lithium methyl carbonate (LMC) or lithium ethyl carbonate (LEC) [24]; these species are believed to be single-electron-induced reduction products of EC. The strong peak between 1050 and 1070 cm^{-1} is characteristic of lithium alkoxides (CH_3OLi and/or CH_3CH_2OLi) that result from electrolyte solvent reduction [25].

In addition to the above, the graphite from $LiPF_6$ cells shows a peak at 837 cm^{-1} that is most likely from $LiPF_6$ residue [23]. The absorptions in the 1040–970 cm^{-1} region indicate the presence of C–O and P–O functional groups from compounds, such as lithium alkyl phosphates and/or lithium fluorophosphates that could result from $LiPF_6$ decomposition [26].

The graphite cycled in $LiF_2BC_2O_4$ shows a high concentration of features in the 1050–950 cm^{-1} region, indicating C–O and B–O functional groups in the SEI. Furthermore, peaks at 1645, 1320, and 773 cm^{-1} (marked by arrowheads) are observed in the $LiF_2BC_2O_4$ sample data. These peaks are characteristic of either lithium oxalates or alkyl esters of oxalic acid [6] that are the products of rearranging reactions of oxalatoborates with lithium alkyl carbonates in the SEI [27]. The peaks may also include small contributions from $LiF_2BC_2O_4$ in the residual electrolyte on the sample surface. Note that peaks from alkyl orthoborates $B(OR)_3$ species around 1364, 1260, and 1041 cm^{-1} [6], observed in graphite samples cycled in LiBOB electrolyte are absent in the $LiF_2BC_2O_4$ sample data. Also note that Li_2CO_3, which has characteristic peaks at 1426 and 870 cm^{-1}, was not found on either sample; that is, Li_2CO_3 can be avoided by careful operation and handling of cells [28].

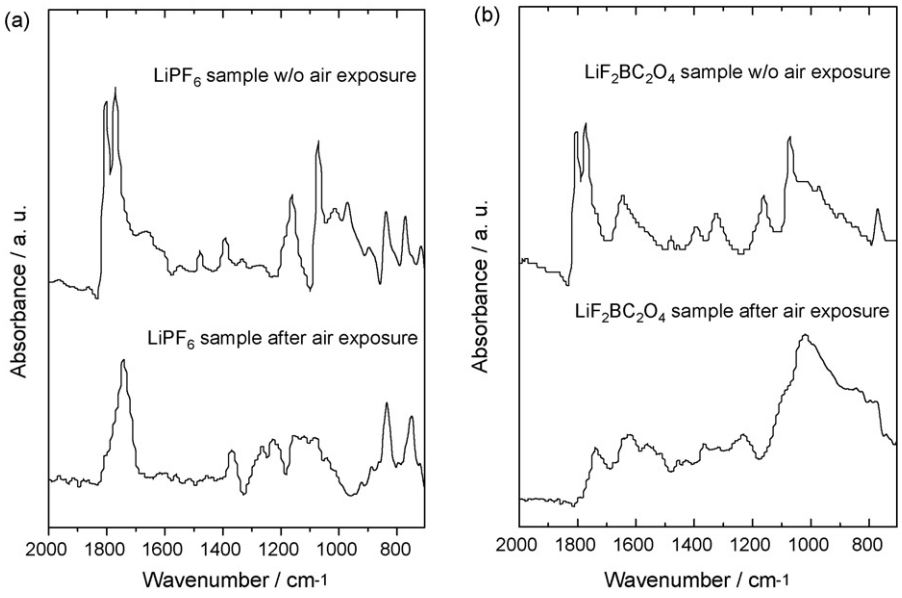

Fig. 6. FTIR data from BF-graphite electrodes, before and after air exposure, cycled in (a) $LiPF_6$- and (b) $LiF_2BC_2O_4$-electrolyte cells.

FTIR-ATR data were also obtained on the above samples after 6 h exposure to ~30% humidity air (see Fig. 6). The changes, seen in the spectra, indicate that the graphite SEI layer is significantly altered on air exposure. These changes include the following: (1) reduction in intensity arising from solvated EC:lithium and lithium alkyl carbonates, the main SEI species; (2) presence of Li_2CO_3, in the SEI of all samples examined, which probably results from reactions between the lithium alkyl carbonate and H_2O and/or CO_2 in air; (3) broad peak at ~1000 cm^{-1} in the $LiF_2BC_2O_4$ sample, probably from inorganic O–B–O linkages, which indirectly indicates the existence of trigonal borates in the SEI; and (4) decrease in intensity of absorptions arising from P–O function groups in the $LiPF_6$ sample SEI.

3.3. XPS

Fig. 7 shows C 1s, F 1s, O 1s, P 2p, and B 1s spectra from the BF-graphite electrodes, cycled once between 2.0 and 0.0 V, in $LiPF_6$- and $LiF_2BC_2O_4$-electrolyte cells; data from pure $LiPF_6$

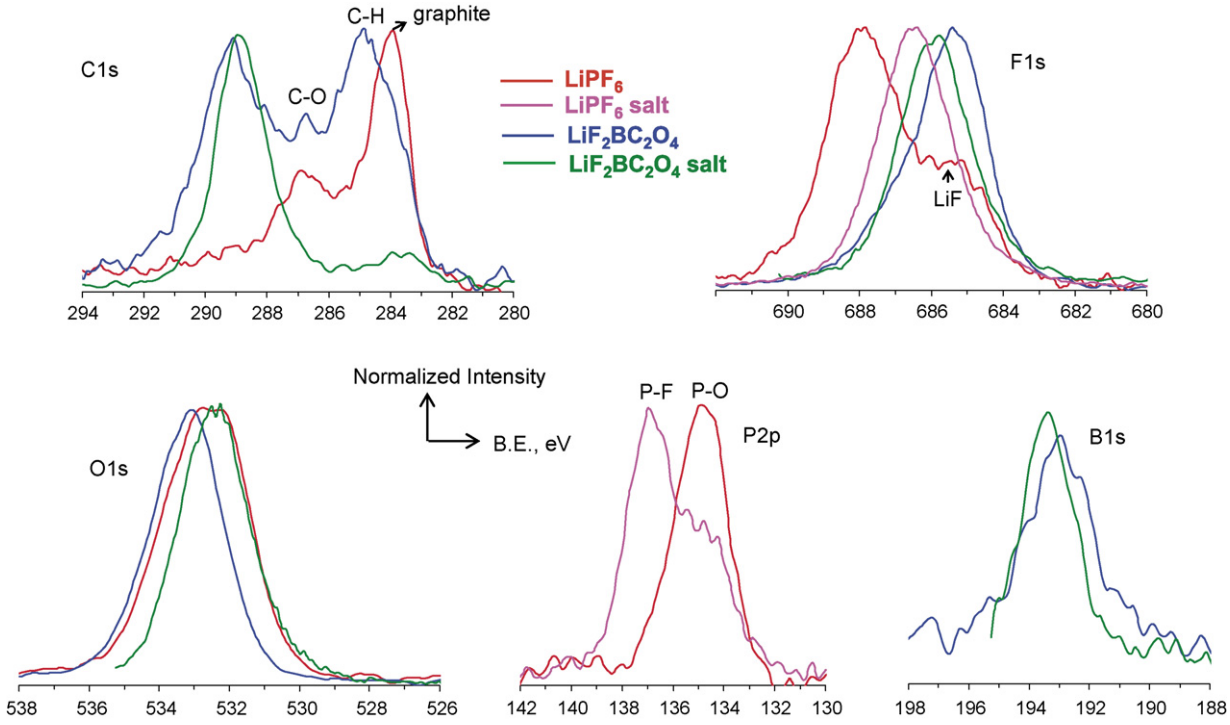

Fig. 7. XPS spectra from electrodes cycled in $LiPF_6$- and $LiF_2BC_2O_4$-electrolyte cells. Reference data from $LiPF_6$ and $LiF_2BC_2O_4$ salts are shown for comparison.

and $LiF_2BC_2O_4$ salts are shown for comparison. The spectral intensities have been normalized to highlight peaks in the data.

The C 1s spectrum for the $LiPF_6$-cell sample shows intensities at 284 eV (C–C from graphite), 284.8 eV (C–H), 286.5 eV (ether linkage, C–O) and in the 288–291 eV range (carbonate, OCO_2). The 284 eV intensity indicates incomplete graphite coverage, and may result from partial SEI dissolution during the delithiation cycle. The 286.5 eV intensity is consistent with the presence of lithium alkoxides (ROLi) suggested by the FTIR data. The intensity in the 288–291 eV range suggests the presence of lithium alkyl carbonates; R–CH_2OCO_2Li shows intensity at 288 eV and R–CH_2OCO_2Li at ~290–291 eV [29]. The hydrocarbons in both lithium alkoxides and lithium alkyl carbonates would contribute to the intensity at 284.8 eV.

In the C 1s spectrum for the $LiF_2BC_2O_4$-cell sample, the dominant peaks are at ~285 and at ~289 eV; significant intensity is also observed at 286.5 eV. The 284 eV intensity is relatively weak, which indicates that the graphite is almost completely covered by the SEI; the data also suggest a thicker SEI on the $LiF_2BC_2O_4$ than on the $LiPF_6$ sample. Lithium oxalate (or alkyl esters of oxalic acid) is probably a major contributor to the ~289 eV peak; the oxalate species in the $LiF_2BC_2O_4$ electrolyte residue may also be a minor contributor. The intensities around 290–291 eV indicate the presence of lithium alkyl carbonates. The $LiF_2BC_2O_4$ sample shows a higher concentration of ether linkages (286.5 eV) and hydrocarbons (284.8 eV) than the $LiPF_6$ sample; the 284.8 eV intensity includes contributions from the alkyl esters, lithium alkoxides, and lithium alkyl carbonates.

In typical composite electrode data, C–F bonds in the PVdF binder contribute to intensity at ~688 eV in the F 1s spectra [3]; absence of PVdF in the electrode makes it easier to interpret the F 1s data from BF-graphite electrodes. The F 1s spectrum of the $LiPF_6$ sample contains $Li_xPO_yF_z$ (~688 eV) and LiF (685.5 eV); $LiPF_6$-bearing electrolyte residue (~686.5 eV) may also contribute to some of the spectral intensity. The dominant peak in the F 1s spectrum from the $LiF_2BC_2O_4$ sample occurs at ~685.5 eV, which appears to be from residual $LiF_2BC_2O_4$ salt; the presence (or absence) of LiF in the SEI could not be determined from the data.

The O 1s spectra for both $LiPF_6$ and $LiF_2BC_2O_4$ samples are similar and consistent with the presence of ether linkages at 533 eV, and lithium alkyl carbonates (R–CH_2OCO_2Li at 532.5 eV and R–CH_2OCO_2Li at ~534 eV). The P 2p spectrum of the $LiPF_6$ sample indicates P–O functional groups arising from $Li_xPO_yF_z$ species in the SEI. The B 1s spectrum of the $LiF_2BC_2O_4$ sample is consistent with the presence of tricoordinated borate species at 192.5 eV; taken along with the ether linkage at 286.5 eV in C 1s and 533 eV in O 1s, the data suggest the existence of trigonal borate oligomers in the $LiF_2BC_2O_4$ sample SEI. Note that B 1s data also include contributions from residual $LiF_2BC_2O_4$ salt. Experiments are in progress to differentiate contributions from the graphite SEI layer components and electrolyte residue on the graphite surface. These studies include (a) examination of electrode surfaces after rinsing in appropriate solvents and (b) studies of the rinsed solutions to determine soluble components of the SEI layer.

4. Summary and conclusions

Binder-free graphite electrodes were prepared by the electrophoretic deposition of SFG-6 graphite on to copper foils in an acetonitrile solution containing small amounts of triethylamine. Electrochemical performance of the electrodes were evaluated in cells containing two types of electrolytes: 1.2 M $LiPF_6$ or 1 M $LiF_2BC_2O_4$ in EC:EMC (3:7, w/w) solvent. The cells exhibited stable cycling performances between 2.0 and 0.0 V at a current density of 8 mA g^{-1}. The graphite SEI layers, formed after a single lithiation–delithiation cycle between 2.0 and 0.0 V in both $LiPF_6$ and $LiF_2BC_2O_4$ electrolytes were examined by FTIR and XPS. The SEI layers from both cells indicated the presence of lithium alkyl carbonates ($ROCO_2Li$) and lithium alkoxides (ROLi); the ROLi content of the $LiF_2BC_2O_4$ cell was higher than that of the $LiPF_6$ cell. In addition, the SEI layer coverage was greater on the $LiF_2BC_2O_4$ sample than on the $LiPF_6$ sample. Furthermore, trigonal borate oligomers are most likely present in the $LiF_2BC_2O_4$ sample SEI, whereas lithium fluorophosphates species are present in the $LiPF_6$ sample SEI. The absence of Li_2CO_3 is noteworthy, and suggests that the presence of this compound in the graphite SEI can be avoided by careful operation and handling of cells. Our data also show that the graphite SEI layer is significantly altered on air exposure, which is consistent with previously reported observations.

Acknowledgements

The authors acknowledge Prof. Koichi Ui of Iwate University for helpful discussion on the graphite film preparation. We are grateful for the assistance of D. Dees and A. Jansen at Argonne National Laboratory and S. Maclaren, R. Haasch, and E. Sammann at the University of Illinois at Urbana-Champaign. The SEM data were obtained at the Center for Microanalysis of Materials at the University of Illinois, which is partially supported by the U.S. Department of Energy under grant DEFG02-96-ER45439. This work was supported by the U.S. Department of Energy, Office of FreedomCar and Vehicle Technologies. The submitted manuscript has been created by UChicago Argonne, LLC, Operator of Argonne National Laboratory ("Argonne"). Argonne, a U.S. Department of Energy Office of Science laboratory, is operated under contract no. DE-AC02-06CH11357. The U.S. Government retains for itself, and others acting on its behalf, a paid-up nonexclusive, irrevocable worldwide license in said article to reproduce, prepare derivative works, distribute copies to the public, and perform publicly and display publicly, by or on behalf of the Government.

References

[1] E. Peled, J. Electrochem. Soc. 126 (1979) 2047.
[2] T. Zheng, A.S. Gozdz, G.G. Amatucci, J. Electrochem. Soc. 146 (1999) 4014.
[3] M. Herstedt, D.P. Abraham, J.B. Kerr, K. Edström, Electrochim. Acta 49 (2004) 5097.
[4] V. Eshkenazi, E. Peled, L. Burstein, D. Golgodnitsky, Solid State Ionics 170 (2004) 83.

[5] H. Herstedt, A.M. Andersson, H. Rensmo, H. Siegbahn, K. Edström, Eletrochim. Acta 49 (2004) 4939.
[6] G.V. Zhuang, K. Xu, T.R. Jow, P.N. Ross Jr., Electrochem. Solid State Lett. 7 (2004) A224.
[7] H. Ota, Y. Sakata, A. Inoue, S. Yamaguchi, J. Electrochem. Soc. 151 (2004) A1659.
[8] G.V. Zhuang, P.N. Ross Jr., Electrochem. Solid State Lett. 6 (2003) A136.
[9] G.V. Zhuang, K. Xu, H. Yang, T.R. Jow, P.N. Ross Jr., J. Phys. Chem. B 109 (2005) 17567.
[10] S.S. Zhang, J. Power Sources 162 (2006) 1379.
[11] A.M. Andersson, D.P. Abraham, R. Haasch, S. MacLaren, J. Liu, K. Amine, J. Electrochem. Soc. 149 (2002) A1358.
[12] D. Aurbach, B. Markovsky, I. Weissman, E. Levi, Y. Ein-Eli, Eletrochim. Acta 45 (1999) 67.
[13] M. Inaba, H. Yoshida, Z. Ogumi, T. Abe, Y. Mizutani, M. Asano, J. Electrochem. Soc. 142 (1995) 20.
[14] D. Bar-Tow, E. Peled, L. Burstein, J. Electrochem. Soc. 146 (1999) 824.
[15] E. Peled, D. Golodnitsky, A. Ulus, V. Yufit, Eletrochim. Acta 50 (2004) 391.
[16] S.S. Zhang, Electrochem. Commun. 8 (2006) 1423.
[17] Z. Chen, J. Liu, K. Amine, Electrochem. Solid State Lett. 10 (2007) A45.
[18] J. Liu, Z. Chen, S. Busking, K. Amine, Electrochem. Commun. 9 (2007) 475.
[19] K. Ui, T. Minami, K. Ishikawa, Y. Idemoto, N. Koura, J. Power Sources 146 (2005) 698.
[20] K. Xu, S. Zhang, T.R. Jow, Electrochem. Solid State Lett. 6 (2003) A117.
[21] M. Wachtler, M. Wohlfahrt-Mehrens, S. Ströbele, J.-C. Panitz, U. Wietelmann, J. Appl. Electrochem. 36 (2006) 1199.
[22] K. Xu, U. Lee, S.S. Zhang, T.R. Jow, J. Electrochem. Soc. 151 (2004) A2106.
[23] S. Geniès, R. Yazami, J. Garden, J.C. Frison, Synth. Met. 93 (1998) 77.
[24] K. Xu, G.V. Zhuang, J.L. Allen, U. Lee, S.S. Zhang, P.N. Ross Jr., T.R. Jow, J. Phys. Chem. B 110 (2006) 7708.
[25] G.V. Zhuang, H. Yang, B. Blizanac, P.N. Ross, Electrochem. Solid State Lett. 8 (2005) A441.
[26] K. Ohwada, Appl. Spectrosc. 22 (1968) 209.
[27] K. Xu, U. Lee, S.S. Zhang, M. Wood, T.R. Jow, Electrochem. Solid State Lett. 6 (2003) A144.
[28] K. Edström, M. Herstedt, D.P. Abraham, J. Power Sources 153 (2006) 380.
[29] A.M. Andersson, PhD Dissertation, Uppsala University, Sweden, 2001.